Limnol. Oceanogr., 52(5), 2007, 1898–1909

Bioturbation and bioirrigation extend the open exchange regions in permeable sediments

N. Volkenborn[1]
Alfred Wegener Institute for Polar and Marine Research, Wadden Sea Station Sylt, Hafenstrasse 43, D-25992 List, Germany

L. Polerecky
Max Planck Institute for Marine Microbiology, Celsiusstrasse 1, D-28359 Bremen, Germany

S. I. C. Hedtkamp[2] *and J. E. E. van Beusekom*
Alfred Wegener Institute for Polar and Marine Research, Wadden Sea Station Sylt, Hafenstrasse 43, D-25992 List, Germany

D. de Beer
Max Planck Institute for Marine Microbiology, Celsiusstrasse 1, D-28359 Bremen, Germany

Abstract

Large-scale experimental exclusion of lugworms (*Arenicola marina*) from 400 m² intertidal fine sand revealed significant effects of their bioturbation and bioirrigation on sediment characteristics, benthic infauna composition, and the dominant mineralization and benthic–pelagic exchange processes in the sediment. Absence of lugworms resulted in sediment clogging with organic-rich fine particles, an eightfold decrease in sediment permeability, low oxygen penetration depths, and accumulation of reduced mineralization products in the pore water. The sand flat inhabited by lugworms had low fine-particle and chlorophyll contents and low sulfide and nutrient concentrations in the pore water. The effects were not limited to the vicinity of lugworm burrows but extended throughout the entire sediment down to ~20-cm depth. Sediments with the lugworm shared the characteristic of low-organic, advection-driven permeable sand rather than of muddy, diffusion-dominated sediments in the absence of lugworms. Areal oxygen uptake rates depended strongly on hydrodynamic conditions: under calm conditions, sedimentary oxygen uptake was slightly higher at the exclusion site. Experimental flushing using controlled hydrodynamic conditions showed that oxygen uptake at the lugworm site would be higher during more dynamic conditions (e.g., storms) due to significantly deeper oxygen penetration permitted by higher sediment permeability. Our results indicate an interactive effect of bioturbating organisms and hydrodynamics on water–sediment exchange processes and highlight the importance of benthic infauna for sedimentary processes even in physically dominated systems.

Biogeochemical cycling and mineralization processes in coastal marine soft sediments are controlled by the interplay of physical variables and the activities of bottom-dwelling organisms (Malcolm and Sivyer 1997; Reise 2002). In exposed porous sand, wave- and current-induced pressure gradients result in advective pore-water flow deep (>20 cm) into the permeable sediment (Huettel et al. 1998; D'Andrea et al. 2002; De Beer et al. 2005). The supply of oxygen to the sediment regulates the distribution of microbial communities (Fenchel and Finlay 1995) and, in turn, organic matter degradation and nutrient cycling (Mackin and Swyder 1989). Despite the low organic content, conversion rates in permeable sand can be high due to efficient input of oxygen and organic matter, and removal of degradation products (Werner et al. 2006).

Macrofaunal activities, i.e., bioturbation and burrow ventilation may become the predominant driver of benthic–pelagic solute and particle exchange in more sheltered, cohesive sediments (Kristensen 1988; Aller 1998; Glud et al. 2003). Recent studies suggest that a significant role of bioturbating and bioirrigating infauna for the sediment–water exchange is not limited to cohesive sediments and not restricted to the vicinity of animal burrows: In permeable

[1] Corresponding author (nils.volkenborn@awi.de).
[2] Present address: Umweltbundesamt, Wörlitzer Platz 1, 06844 Dessau, Germany.

Acknowledgments

We thank Tanya Romanova and Birgit Hussel for assistance with nutrient and carbon and nitrogen (CN) analyses, Gaby Eickert for preparation of microsensors, Martina Löbl, Anett Matthäi, and Simone Böer for help in the field and laboratory, and Reimer Magens for sharing his technical knowledge. Valuable comments by Karsten Reise, Stefan Forster, Ronnie Nøhr Glud and one anonymous reviewer are greatly appreciated.

The study was supported by the Alfred Wegener Institute for Polar and Marine Research in the Helmholtz Association and the Max Planck Society. Additional funding during preparation of this manuscript was provided by the German Ministry for Education and Research and the State of Bremen through funding of the project Netherlands Bremen Oceanography (NEBROC), and the E.U. project COSA ("Coastal sands as biocatalytical filters," EVK3-CT2002-0076). The authors also acknowledge the support by the EU-Network Marine Biodiversity and Ecosystem Functioning (MARBEF), which is funded in the Community's Sixth Framework Programme (contract GOCE-CT-2003-505446).

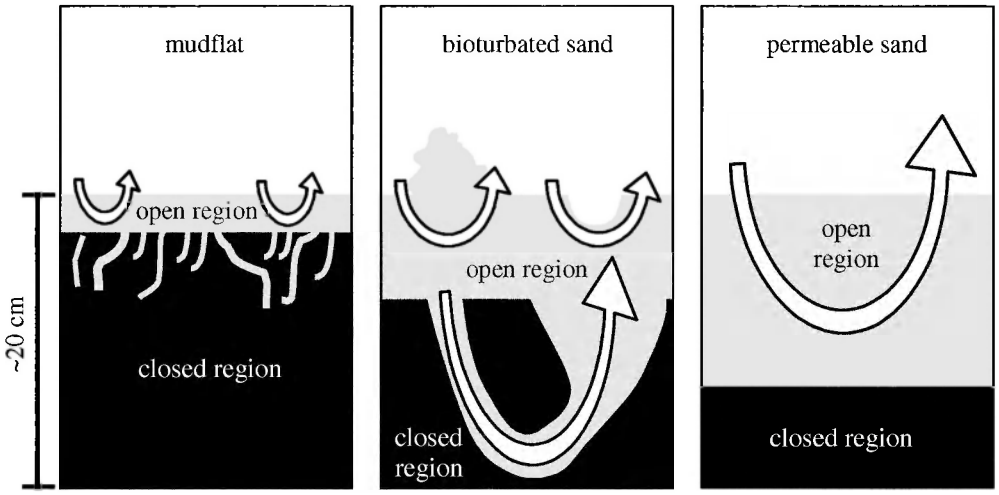

Fig. 1. Schematic diagram depicting the hypothesized extension of the open-exchange regions in permeable sand by bioturbating and bioirrigating infauna. The permeable sand and the mudflat constitute the two extreme types of intertidal flats. Sediment–water exchange processes in permeable sand are driven by physical advection, while exchange processes in mud flats are limited to a thin sediment surface layer and macrofaunal burrows. The greater volume of the open regions (gray) in the presence of bioturbating infauna is caused by the bioirrigation of the sediment and by an increased advective flushing, facilitated by high sediment permeability and intensified roughness of the bioturbated seabed.

sand, macroinfauna pump water across the burrow wall inducing advective pore-water flow through the surrounding sediment (Wethey and Woodin 2005; Timmermann et al. 2006). Bioturbation of the seafloor often results in a pit-and-mound topography at the sediment surface which generates pore-water pressure gradients under flow conditions that drive advective pore-water flow through the permeable sand (Huettel and Gust 1992). The selective ejection of fine-grained material into the water column may furthermore increase the bulk sediment permeability of the inhabited area (Ziebis et al. 1996). Thus, the combined direct and indirect effects of bioturbation and bioirrigation may considerably affect overall exchange rates between inhabited sediment and the overlying water.

The advective input of oxygen as the most energetically favorable electron acceptor strongly affects rates of organic matter degradation in marine sediments (Thamdrup and Canfield 2000). The permeable seabed can be vertically divided into an open region, where the solute exchange is rapid due to physically and biologically driven advective pore-water flow, and a closed region, where comparably slow exchange is governed by diffusion (Fig. 1). It can be speculated that dense populations of bioturbating macroinvertebrates can significantly extend the open exchange regions by their own bioirrigation, by maintaining the sediment permeability, and by creating a pit-and-mound topography of the sediment surface. Manipulated laboratory microcosms are a commonly used approach for the study of the effects of macrofauna on benthic metabolism and sediment–water exchange (e.g., Banta et al. 1999), but the exclusion of physical forces has been shown to affect the magnitude of macrofaunal effects (Papaspyrou et al. 2007). In situ experimental works remain few (Huettel 1990; D'Andrea et al. 2002), presumably due to difficulties in manipulating species composition and measuring oxygen fluxes in an open and fluid system (Biles et al. 2002). Moreover, small-scale approaches may alleviate possible effects of macrofaunal activities due to lateral particle and pore-water exchange between manipulated plots and the surrounding sediment, especially in dynamic environments like intertidal sand flats.

Here, we present a large-scale experimental in situ approach to explore the effects of bioturbating lugworms (*Arenicola marina*) on physical sediment properties and geochemical exchange processes in intertidal fine sand. Deposit-feeding lugworms are the dominant large burrowing macrofaunal species and consequently the major source of sediment bioturbation and bioirrigation in intertidal sediments of the Wadden Sea (North Sea, Europe). They rework large amounts of sediment, create a characteristic pit-and-mound topography at the sediment surface, and actively irrigate their J-shaped burrows (review by Riisgård and Banta 1998). Since defecation occurs at the sediment surface, and tides and waves spread out the feces mounds over the entire sediment surface during submersion, we hypothesize an increased resuspension of fine particles, which will ultimately lead to a significant loss of fine material from lugworm-populated areas and a larger permeability enhancing sediment–water exchange processes.

We speculate that even in physically dominated systems, macrofaunal activities may considerably affect benthic–pelagic exchange processes. Based on this speculation, we conducted experiments on a 400 m^2 lugworm-exclusion area and the adjacent lugworm-inhabited sediment, situated in the low intertidal and on a nearby permeable sand in the shallow subtidal zone. Two years after lugworms were excluded, we analyzed sediment and pore-water characteristics at the three sites. Furthermore, we de-

termined oxygen exchange rates using the combination of ex situ oxygen optode imaging, in situ microsensor oxygen profiling, and sediment core incubations. Our goal was to identify whether differences in sediment characteristics at the lugworm and the exclusion sites affect benthic–pelagic exchange processes of the inhabited sediment under varying physical conditions of intertidal sand flats.

Methods

Study site and lugworm-exclusion area—The study was conducted on a sand flat in a sheltered bay (55°02′N, 08°26′E) near the island of Sylt, Germany. In 2002, a large-scale, long-term lugworm exclusion experiment was commenced by inserting a 1-mm meshed net 10-cm deep into the sediment, blocking the burrows of *A. marina* over an area of 400 m^2. The large size of the experimental plots was chosen to minimize effects of lateral sediment transport typical of sandy intertidal flats. For control, an area of the same size next to the exclusion plot was disturbed with a backhoe in the same way, but without inserting the net. Lugworms were permanently excluded by the net, while abundances remained 20–30 individuals (ind.) m^{-2} at the control site (Volkenborn and Reise 2006).

A. marina lives in 20–40-cm-deep J-shaped burrows, ending in a U-shape with a vertical head shaft through which surface sediment slides down, is ingested by the worm, and defecated as a fecal mound at the sediment surface above the tail shaft. Selective feeding by lugworms on small particles (<80 μm) results in the formation of a coarse shell debris layer in the feeding depth of ~20 cm (Hylleberg 1975). For respiration, oxygen-rich surface water is pumped through the tail shaft into the burrow and subsequently through the permeable walls of the feeding pocket and into the surrounding sediment by means of peristaltic movements (review by Riisgård and Banta 1998). Roughly 90% of the total 4,300-km^2 intertidal area of the Wadden Sea consists of "lugworm flats," populated by 20–40 ind. m^{-2}. Abundances are low to zero in soft mud, and also in clean, unstable sand exposed to strong currents or waves near the low water line and below (Beukema 1976; Reise 1985).

The measurements presented here were conducted on the exclusion and the control plots two years after the experimental setup. Sediments at the study site are moderately sorted fine sand with a median particle size of 230 μm. Additional investigations were done at a nearby (2 km) subtidal site with an advective-driven permeable sand, composed of moderately well– to well-sorted medium sand with a median grain size of 340 μm (De Beer et al. 2005; Werner et al. 2006). Salinity at all sites varies on average between 27.5 in spring and 31 in summer, and freshwater upwelling is negligible. Mean tidal range is 1.8 m. Emersion time of intertidal experimental plots in the intertidal is ~3–4 h per tide. Tidal currents are the dominant hydrodynamic force, but wave action becomes important when winds blow from northern and eastern directions. Further details regarding sediment characteristics and biota at the study site are provided by Austen (1994) and Reise (1985). Since the aim of the present study was to analyze the effects of a dominant bioturbator on the biogeochemistry of marine sands beyond the vicinity of burrows, all sampling and measurements at the lugworm site were done ≥10 cm apart from the nearest lugworm cast or funnel.

Solid-phase analysis—Samples for sediment and pore-water analyses were taken randomly from the central part of the experimental plots and at least 10 cm away from lugworm casts or funnels. From each site, four parallel cores (10 cm^2, 10-cm depth) were taken for sediment analysis. After homogenizing 1-cm slices from the parallel cores, three subsamples of ~3 g were taken from each depth, freeze dried, and kept at −20°C until further handling. The rest of the sediment was used for pore-water extraction by blowing with pressurized nitrogen gas (see following). Two of the freeze-dried subsamples were used for the determination of particulate organic carbon : particulate organic nitrogen (POC : PON) and chlorophyll *a* (Chl *a*) content, which was done in triplicate. For the determination of particulate organic matter, 75 mg of homogenized sediment was treated with 1 mol L^{-1} HCl to remove carbonates, dried (1 h, 70°C), and analyzed with a C : N analyzer (Thermo-Finnigan Flash EA 1112). Chl *a* concentrations were measured spectrophotometrically according to Lorenzen (1967) using supernatant obtained by centrifugation (5 min at 4,000 rpm) of 1-g sediment samples extracted in 10-mL acetone (90%) overnight at 4°C. The third freeze-dried subsample from the exclusion and lugworm site was used for grain-size analysis using a laser particle sizer. Prior to the analysis, samples were treated with acetic acid (30%) to remove carbonate particles, with hydrogen peroxide (30%) to remove organic compounds, and with ultrasonic to separate associated particles. The fine fraction was additionally estimated by dry sieving samples pooled from 20 locations within each plot taken with a 2-cm^2 core to 5-cm depth. Sediment permeability was estimated by the constant head method (Klute and Dirksen 1986). From each site, three 10-cm^2 cores (~8-cm depth) were taken, and the time needed for the passage of 1 mL of seawater was measured under four different hydrostatic pressures, ranging from a 5-cm to 30-cm water column (0.5–3.0 kPa).

Pore-water extraction and analysis—Multiple pore-water samples were collected simultaneously with a "pore-water lance" from six different depths (3, 5, 7, 10, 15, and 20 cm) while maintaining anaerobic conditions (Huettel 1990). A polyvinylchloride (PVC) plate at the sediment surface was used to prevent intrusion and mixing with the overlying water, and a steel tip allowed penetration of the net and sampling of sediment layers deeper than 10 cm. From each of four randomly chosen locations within one experimental plot, ~5 mL of pore water was retrieved. The first 2 mL was discarded to rinse the tygon tubing. The pooled 20-mL samples were filtered (0.45-μm nylon filter) and frozen at −20°C (for phosphate and ammonium analyses) or stored dark at 4°C (silicate analysis) until measurements were taken with an autoanalyzer (AA_3, Bran & Luebbe). Sampling was done in October 2003 and April and July 2004. In July 2004, sulfide concentrations in the pore water

were measured with the colorimetric methylene blue method (Fonselius 1983). Sampling with the pore-water lance was only successful in the intertidal area (exclusion and lugworm plots).

A second pore-water extraction method was based on blowing out pore water with pressurized N_2 gas. This method was applied for all sites and enabled pore-water extraction with higher spatial resolution. One-centimeter slices from four parallel cores (10 cm^2) from each site were pooled. Pore-water samples of ~5 mL were obtained and analyzed as described above.

Planar optode measurements (ex situ)—Depth profiles of volumetric oxygen consumption rates in the sediment were determined by the flow-through method (Polerecky et al. 2005). The employed planar oxygen optodes (Glud et al. 1996) and the luminescence lifetime measuring system (Holst and Grunwald 2001) allowed the determination of oxygen concentrations and consumption rates with high spatial resolution and in two dimensions (2D).

In June 2004, five parallel cores from the exclusion and four parallel cores from the lugworm plot were investigated with the flow-through technique. The sampling cores, equipped with planar oxygen optodes, had a surface area of 7.5 × 7.5 cm. Sediment was sampled to a depth of 10 cm. Cores were percolated with in situ seawater under pressures ranging from 0- cm to 50-cm water column (0–5 kPa). After oxygen distribution reached a steady state, percolation was stopped, and oxygen images were recorded every 10 s. The initial images allowed quantification of oxygen penetration depth at a given hydrostatic pressure. Sedimentary volumetric oxygen consumption rates (OCR_v, expressed per volume of pore water) were calculated as described in Polerecky et al. (2005). Due to low permeability of the exclusion site sediment, a vacuum pump was used to increase the hydrostatic pressure in order to reach deeper oxygen penetration and thus allow quantification of OCR_v in deeper sediment layers. OCR_v rates were averaged in a horizontal direction, resulting in high spatial resolution depth profiles of potential volumetric oxygen consumption rates (denoted as $OCR_v[z]$). Using the oxygen penetration depth, z_p, measured in situ by the microprofiler (see below), areal oxygen consumption rates (OCR_a) were calculated as

$$OCR_a(z_p) = \int_0^{z_p} \phi OCR_v(z) dz. \quad (1)$$

Sediment porosity, ϕ, which was used to express the $OCR_v(z)$ values per volume of sediment, was estimated from 1-cm sediment slices taken from sampling cores to a depth of 5 cm by determining the weight loss after drying the sediment at 60°C.

Sediment core incubation (ex situ)—Independent measurements of oxygen fluxes over the sediment–water interface were done using sediment core incubations. Plexiglas cores with a diameter of 8.3 cm were taken to a depth of ~10 cm and were brought to the nearby laboratory and left overnight in a water bath (150 liters) with site water at in situ temperature (12°C). Sealed cores were submerged with 0.8 liters of site water, and a magnetically coupled stirring system in each core was suspended ~6 cm above the sediment surface, rotating at 50–60 rpm. To determine areal oxygen consumption and photosynthesis rates, sediment cores were incubated in the dark and in the light, respectively, for ~5 h while oxygen concentrations were measured in the overlying water. Water samples (50 mL), analyzed by Winkler titration, were taken 1, 3, and 5 h after the incubation started with a syringe and replaced by air-saturated site water. Since the illumination intensity in the light incubations varied between 20 and 30 μmol photons m^{-2} s^{-1} (measured 1 cm above the sediment surface by a LI-COR Quantum Sensor UF-SQS/L), the light oxygen fluxes were normalized to 30 μmol photons m^{-2} s^{-1}, assuming a linear relationship between the light intensity and oxygen production for the observed intensity range. At the end of each incubation, Chl *a* content in the top centimeter was estimated, and cores were sieved through a 500-μm mesh for the identification of macrofauna species. Their biomass was determined as ash-free dry weight. Sediment core incubations were done in April 2004 using four cores from the exclusion site and three cores from the lugworm and subtidal sites.

Microsensor measurements (in situ)—Large infauna and hydrodynamic forcing considerably influence the in situ sedimentary oxygen consumption. These phenomena are, however, excluded or difficult to mimic in core incubation measurements (Huettel and Gust 1992; Glud et al. 2003). To quantify OCR_a, we therefore additionally combined in situ oxygen penetration depths measured by microsensors and volumetric oxygen consumption rates revealed by planar oxygen optode imaging (see above). Microsensor measurements were done with an autonomous profiler. Day and night profiles from exclusion and lugworm plots were measured continuously in 20-min intervals during the submersion period (~10 h) in April 2004. For daytime measurements, the autonomous profiler was equipped with two Clark-type oxygen microelectrodes (Revsbech 1989). During the night, a sulfide microsensor (Jeroschewski et al. 1996) was added. Profiling was done in 150-μm steps to a depth of 10 cm. Approximately 20 profiles were obtained with each microsensor during one submersion period from which oxygen penetration depths (z_p) and sulfide distributions were determined as a function of time.

Macrofauna sampling—Macrofauna sampling at the intertidal sites was done by counting animals retained with a 1-mm sieve from eight randomly chosen cores (area of 100 cm^2, depth of 10 cm). Sampling at the subtidal station was done from a ship using a 14 × 14 cm box-core. Six parallel cores to a depth of ~15 cm were taken and sieved through a 500-μm mesh. Macrofauna sampling was done in August 2002, 2003, and 2004.

Statistical analysis—One factorial analysis of variance (ANOVA) was applied to test for differences of sedimentary oxygen fluxes, chlorophyll content, and macrobenthic biomass among the three sites in sediment core incubations. Data were square-root transformed to

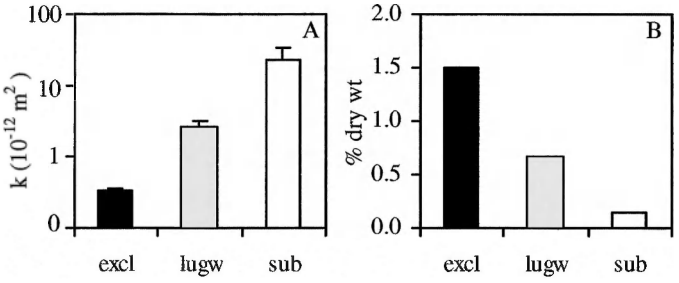

Fig. 2. (A) Sediment permeability and (B) weight proportion of the particles <63 μm in the top 5 cm of the sediment layer at the exclusion (excl), lugworm (lugw), and subtidal (subt) sites (note log *y*-axis in A).

achieve homogeneity of variances (Cochran's test). Post-hoc tests were done using the Tukey honestly significant difference (HSD) procedure on a $p < 0.05$ level. Macrobenthic community response to the experimental treatments in the intertidal was analyzed by univariate ANOVA analysis of (log + 1)–transformed abundance data and multivariate similarity percentages (SIMPER) procedures (using the software package PRIMER v5).

Results

Solid-phase analysis—Sediment characteristics differed significantly between sites. Sediment permeability at the lugworm plot (2.6×10^{-12} m^2) was eightfold higher than at the exclusion plot (0.3×10^{-12} m^2). The highest permeability was found in the subtidal sand (23.4×10^{-12} m^2), which was nine times more permeable than the sediment at the lugworm plots and ~70 times more permeable than the sediment from the exclusion site (Fig. 2A). The amount of fine particles (<63 μm) in the top 5 cm of the sediment was highest at the exclusion (1.5 wt%), medium at the lugworm (0.66%), and lowest at the subtidal station (0.14%, Fig. 2B). The distribution of the fine fraction (Fig. 3A) was significantly positively correlated with the distribution of particulate organic carbon (Fig. 3B) ($r^2 = 0.933$; $p < 0.001$). Fine particles and associated organic material were rather homogenously distributed over the top 15 cm on the lugworm and the subtidal site, slightly decreasing with depth, while sediment from the exclusion plot showed a clear horizontal stratification with fivefold higher values at the sediment surface and twofold higher values between 4-cm and 7-cm depth. Chl *a* concentrations were highest in surface sediment of the exclusion plot (~40 μg g^{-1} dry sediment), compared to less than 20 μg g^{-1} dry sediment on the lugworm and the subtidal plots (Fig. 3C). In the sediment from the subtidal station, high concentrations of Chl *a* were found to a depth of 5 cm, while Chl *a* concentrations in the intertidal were concentrated in the top centimeter. Assuming a POC : Chl *a* ratio of 60 (De Jonge 1980), microphytobenthos made up ~25% of the total POC in the top centimeter of the intertidal sites, and more than 50% at the subtidal site (Fig. 3D).

Pore-water analysis—The presence of lugworms strongly affected pore-water nutrient concentrations. Pore-water

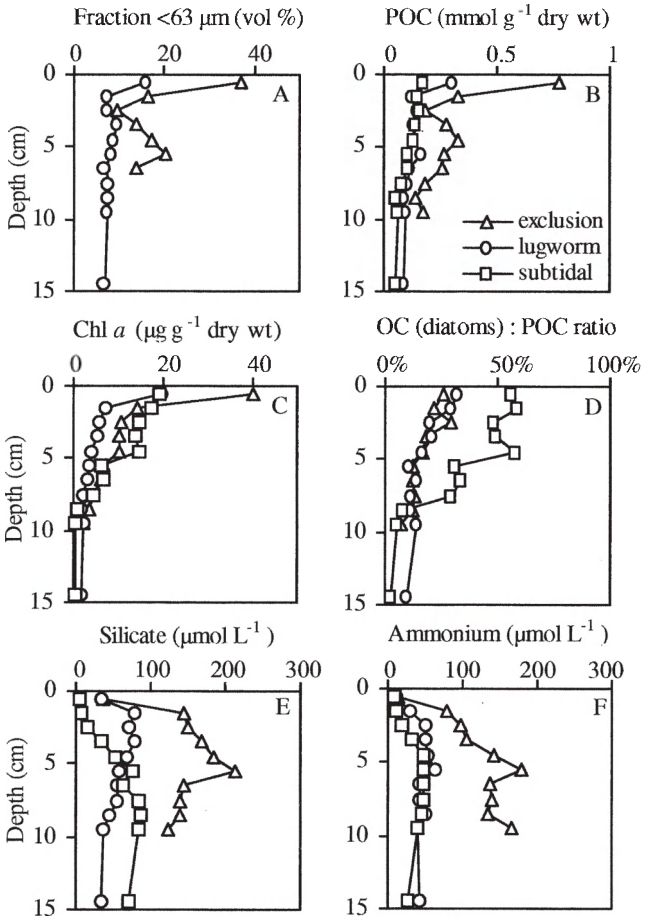

Fig. 3. (A–D) Solid-phase and (E–F) pore-water characteristics of the sediment from exclusion, lugworm, and subtidal sites. The fraction <63 μm was determined by laser particle sizing. Pore-water samples were extracted at the three sites in April 2004 by flushing with pressurized N_2.

extraction with pressurized N_2 enabled the characterization of silicate and ammonia profiles with high vertical resolution for the top 10 cm at all three sites (Fig. 3E,F). At the exclusion site, silicate and ammonia concentrations were more than twofold higher throughout the upper 10 cm compared to the lugworm and the subtidal sites. An additional characteristic of the exclusion site was concentration peaks in ~6-cm depths of >200 μmol L^{-1} silicate and >150 μmol L^{-1} ammonia.

The profiles obtained by the pore-water lance sampling technique indicated a deep flushing effect of *A. marina* (Fig. 4). Nutrient profiles on the exclusion plot exhibited an almost linear increase from 7 cm downward, reaching maximum concentrations of ammonium, phosphate, and silicate of 400, 30, and 270 μmol L^{-1}, respectively, at a depth of 20 cm. In contrast, maximum concentrations of ammonium, phosphate, and silicate on the lugworm plot were found at depths of 5–7 cm. Accumulation of nutrients in the absence of lugworms was evident during all seasons (Fig. 4).

Sulfide concentrations on the lugworm site were below 20 μmol L^{-1} at all depths, while high sulfide concentra-

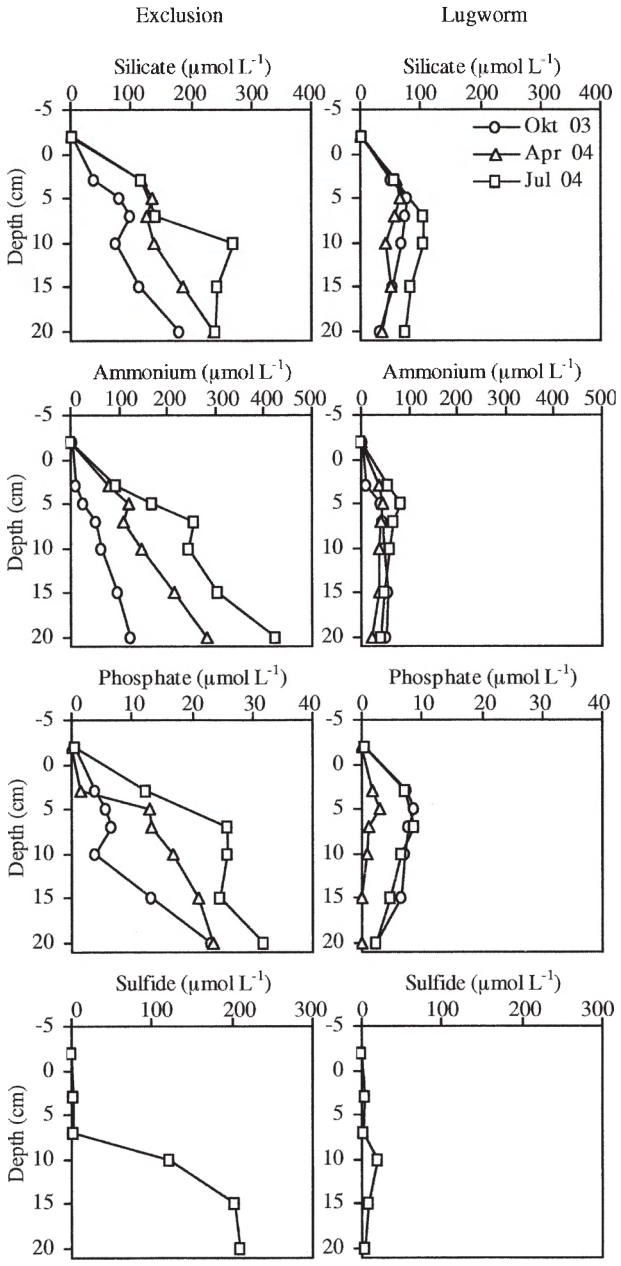

Fig. 4. Nutrient profiles in different seasons obtained with a pore-water lance. Values represent averages from pooled samples taken at four different locations within each site. High nutrient and sulfide concentrations at the exclusion site indicate the deep flushing effect of lugworms.

tions were encountered on the exclusion plot, reaching concentrations of more than 200 μmol L^{-1} below 10-cm depth. Microsensor measurements revealed high sulfide concentrations (up to 150 μmol L^{-1}) below 6-cm depth at the exclusion site directly after submersion and below 8-cm depth during high water and thereafter (profiles not shown). Over the entire tidal cycle, moderate sulfide concentrations (20–50 μmol L^{-1}) were additionally detected at depths of 2–8 cm. At the lugworm site, no sulfide was detected.

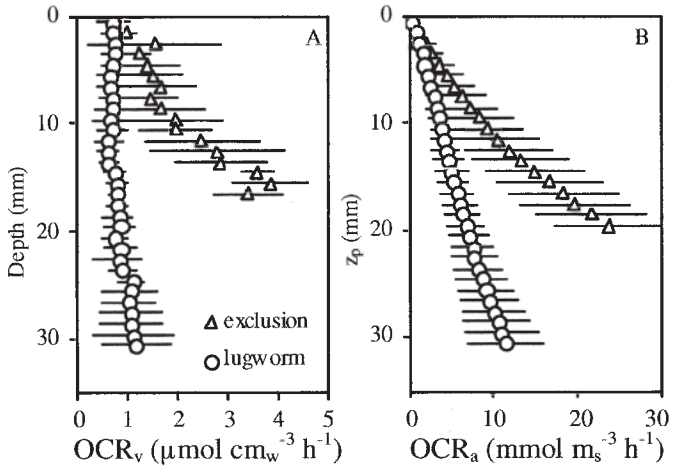

Fig. 5. (A) Depth profiles of volumetric OCR expressed per cm^3 of pore water measured by the flow-through method. (B) Areal OCR as a function of oxygen penetration depth calculated from (A) using Eq. 1. Both profiles indicate much higher potential oxygen consumption at the exclusion site.

Oxygen consumption rates—Depth profiles of potential OCR_v obtained from the planar optode imaging data (oxygen images not shown) are shown in Fig. 5A. The rates on the lugworm plot ranged from 0.6 to 1.5 μmol cm^{-3} h^{-1} and were almost constant in the top 20 mm. OCR_v in the sediment from the exclusion site steeply increased with depth. In the top 2 mm, average OCR_v values were ~0.6 μmol cm^{-3} h^{-1} and comparable to OCR_v on the lugworm site, but they reached rates of up to 4.2 μmol cm^{-3} h^{-1} at a depth of 15 mm. Higher standard deviations also indicated a much higher horizontal variability of OCR_v at the exclusion site.

Using the depth profiles of OCR_v and Eq. 1, potential OCR_a values were calculated as a function of oxygen penetration depth (Fig. 5B). The increase of potential OCR_a with depth was much stronger on the exclusion plot than on the lugworm plot. For the upper 10 mm, the potential OCR_a were the same at the two plots. However, for $z_p > 10$ mm, the exclusion plot showed significantly higher potential OCR_a.

When the oxygen penetration depths at various hydrostatic pressures (Fig. 6A) are combined with the depth profiles of OCR_v (Fig. 5A) in Eq. 1, it is found that, at a given pressure, the sediment from the lugworm site has a much higher potential for oxygen uptake than the sediment from the exclusion site (Fig. 6B). This may sound somewhat surprising, since OCR_a at the exclusion site increased more steeply with z_p than at the lugworm site (Fig. 5B). The explanation is that, under the same hydrostatic pressure, the lower OCR_v rates at the lugworm site are compensated by a much greater volume of flushed sediment facilitated by higher sediment permeability.

In the dark, oxygen uptake rates measured by sediment core incubations were significantly different ($F_{2,9} = 11.46$; $p < 0.01$) among the three sites (Table 1). The oxygen fluxes at the subtidal site (0.79 ± 0.04 mmol m^{-2} h^{-1}) were significantly lower than at the exclusion site (1.4 ± 0.3 mmol m^{-2} h^{-1}; Tukey HSD test, $p < 0.01$) but only

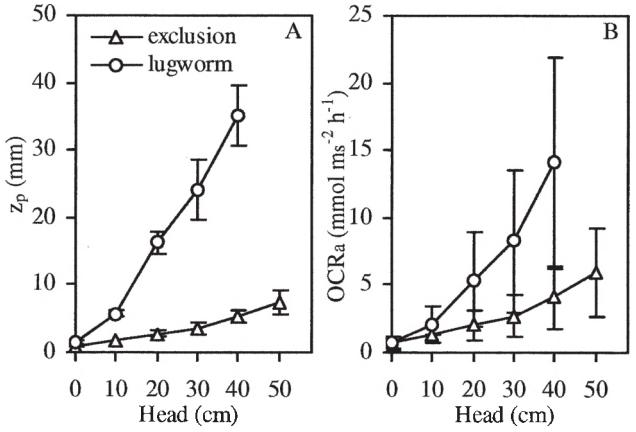

Fig. 6. (A) Oxygen penetration depth and (B) areal oxygen consumption rates as a function of hydrostatic pressure revealed by planar optode imaging. Data in (A) were extracted from images in Fig. 7, while data in (B) were calculated by combining values in (A) and the measured volumetric oxygen consumption rates (Fig. 5A). With increasing hydrostatic pressures, higher oxygen penetration at the lugworm site overcompensates the lower volumetric OCR, resulting in higher areal OCR.

slightly lower than at the lugworm site (1.15 ± 0.09 mmol m^{-2} h^{-1}; Tukey HSD test, $p > 0.05$). Oxygen fluxes during daytime were spatially much more variable than dark fluxes and not significantly different between the sites. Gross photosynthetic oxygen production was very similar in all plots (2.2–2.4 mmol m^{-2} h^{-1}).

Oxygen penetration into sediment and in situ areal oxygen consumption rates—Ex situ steady-state oxygen distributions obtained by optode imaging during the percolation of the sediment cores with aerated seawater demonstrated that oxygen penetration, at a given pressure head, was clearly deeper in the sediment from the lugworm site (Fig. 7). This is quantitatively shown in Fig. 6A. The primary reason for this observation was the significantly higher permeability of the sediment in the lugworm site, which allowed higher flow rates of water through the sediment and thus more efficient delivery of oxygen by advection. Images in Fig. 7 also indicate that the pressure-induced water flow occurred preferentially in channels, indicating inhomogeneities in sediment permeability caused by the presence of polychaete burrows.

In situ oxygen and sulfide microprofiles were measured in April 2004 at the exclusion and lugworm sites during a period of calm and sunny days. No clear differences in oxygen penetration depth were observed between day and night, nor between ebb and flood measurements at both sites (Fig. 8A). On many occasions, the shape of profiles indicated bioirrigation events, resulting in subsurface oxygen concentration peaks and increased oxygen penetration depths. These events were more frequent at the lugworm site, where approximately half of the profiles had increased oxygen penetration depth up to 20 mm, whereas less than 10% of profiles at the exclusion site were affected. Oxygen penetration depth was higher and temporarily more variable at the lugworm site (13.0 ± 6.6 mm) than at the exclusion site (9.3 ± 4.9 mm).

Combining the in situ time series of oxygen penetration (Fig. 8A) and the planar optode measurements of OCR_v (Fig. 5A), OCR_a values were calculated for both experimental sites (Fig. 8B). Overall, OCR_a was temporarily more variable at the lugworm site (2.4–7.2 mmol m^{-2} h^{-1}) than at the exclusion site (4.8–9.0 mmol m^{-2} h^{-1}). At the exclusion site, two bursts of OCR_a were the result of the deep oxygen penetration due to macrofauna activity (*see* Fig. 8A). During times of low variability, i.e., when the profiles were not affected by bioirrigation (e.g., the first 4 h), OCR_a was threefold higher at the exclusion site.

Table 1. Diffusive oxygen fluxes across the sediment–water interface in the light (at 30 μmol photons m^{-2} s^{-1}) and in the dark based on sediment core incubation measurements. Gross photosynthetic oxygen production was calculated as the difference between the light and dark fluxes. Negative values indicate fluxes from the water into the sediment. Mean values and standard deviations (SD) were obtained from $n=4$ (exclusion), $n=3$ (lugworm), and $n=3$ (subtidal) replicate measurements. Values of macrofauna biomass (ash-free dry weight; AFDW) and Chl *a* content in the sediment indicate that the lugworm tidal flat combines the high secondary production of the lugworm exclusion site with the low microphytobenthic biomass in the subtidal sediment.

	Exclusion (mean±SD)	Lugworm (mean±SD)	Subtidal (mean±SD)
Light flux (mmol m^{-2} h^{-1})	0.83±0.57	1.24±0.59	1.57±0.36
Dark flux (mmol m^{-2} h^{-1})	−1.38±0.26	−1.15±0.09	−0.79±0.04
Gross photosynthetic oxygen production (mmol m^{-2} h^{-1})	2.21±0.46	2.40±0.55	2.36±0.35
AFDW (g m^{-2})	11.4±6.4	12.4±8.8	1.4±1.9
Chl *a* (μg g^{-1})	29.9±7.23	16.5±0.6	16.5±1.2

Macrofauna—In the course of the experiment, the macrobenthic community at all three sites was dominated by a small number of species (Table 2). The species composition considerably differed among years and sites. In the first year, adult *Nereis* (*Hediste*) *diversicolor* and tube-building polychaetes *Pygospio elegans* and *Polydora cornuta* settled preferentially on lugworm exclusion plots. The lugworm site was dominated by free-burrowing oligochaetes (*Tubificoides benedii*) and polychaetes (*Scoloplos* cf. *armiger*). This shift in the benthic community from free-burrowing species in the presence of lugworms to tube-building species in the absence of lugworms was also evident in the following years. At the subtidal site, the free-burrowing species *Scoloplos* cf. *armiger* and *Spio martinensis* without a permanent burrow system were the dominating species in all years. Macrofauna biomass at the intertidal sites was almost tenfold and significantly higher than at the subtidal site (Tukey HSD test, $p < 0.05$).

Discussion

Large-scale exclusion of the lugworm *A. marina* from intertidal fine sand resulted in the clogging of the sediment

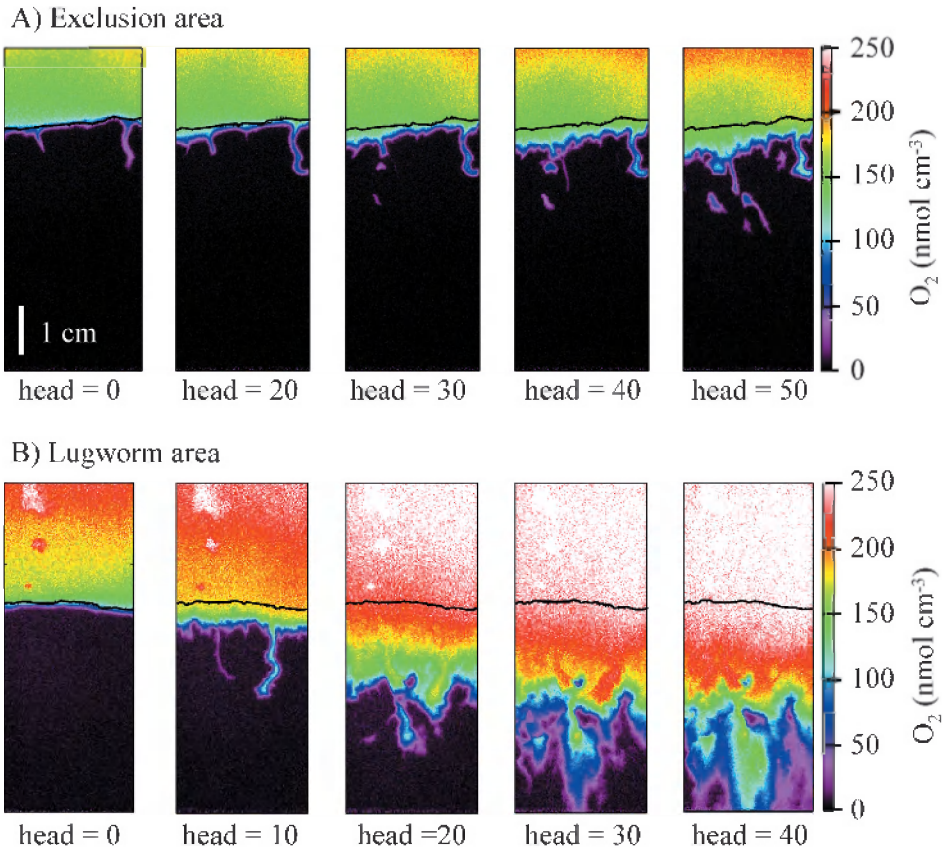

Fig. 7. Steady-state oxygen distributions at different hydrostatic pressures (pressure head in cm H_2O) in sediment from the (A) exclusion and (B) lugworm plots measured in a core equipped with a planar oxygen optode. The black horizontal lines indicate the sediment surface. With increasing hydrostatic pressures, oxygen penetration in the permeable sediment from the lugworm site was much easier than in the sediment from the exclusion site.

matrix with fine particles and associated organic material and a significant decrease of sediment permeability (from 2.6×10^{-12} m^2 to 0.33×10^{-12} m^2, which is lower than the minimum value of $1-1.5 \times 10^{-12}$ m^2 needed for significant advective water exchange; Huettel and Gust 1992). Lugworm exclusion and the associated decrease in sediment permeability resulted in an accumulation of mineralization products in the pore water. Conversely, lugworm presence inhibited these intertidal sand-flat developments. Assuming diffusion-dominated mudflats (with a relatively narrow open region) and advection-dominated permeable sand (with a wider open region) as two extreme types of intertidal flats, our large-scale exclusion experiment indicates that lugworms are responsible for maintaining a sandy and permeable habitat. Lugworms increase the volume of the open region by preserving sediment permeability, by their own bioventilation, and by sustaining a habitat that favors other bioirrigating species and inhibits tube-building infauna.

Pore-water profiles of phosphate, silicate, and ammonium indicated an efficient removal of degradation products in the sediment inhabited by the lugworm. The depletion of nutrients was evident in different depths and several centimeters away from lugworm burrows, indicating that the effects of lugworm presence on pore-water chemistry are not limited to the areas adjacent to their burrows but may affect the characteristics of the entire permeable sediment (at least of the top 20 cm investigated in this study).

The presence of *A. marina* inhibited the accumulation of fine particles and associated organic material, presumably as a result of continuous bioturbation of the sand flat. Lugworm abundances at our study site correspond to a reworked sediment layer of ~10 cm yr^{-1} (Cadée 1976). Due to their greater chance of being swallowed, small particles are preferentially deposited onto the sediment surface within the fecal casts (Hylleberg 1975). Although the casts of *Arenicola* may persist over several tidal cycles under calm conditions, they are often washed away by waves and currents within minutes after submersion under windy conditions. This may possibly be the leading mechanism resulting in a significant loss of the fine fraction from the sediment and in the maintenance of high sediment permeability.

Lugworms reduced the biomass of microphytobenthos. Benthic microalgae play a major role in the sediment dynamics of intertidal sand flats (Paterson 1989) and affect the frequency and magnitude of erosion events (Grant et al. 1986). Extrapolymeric substances excreted by benthic diatoms trap fine particles and stabilize sediments (Yallop

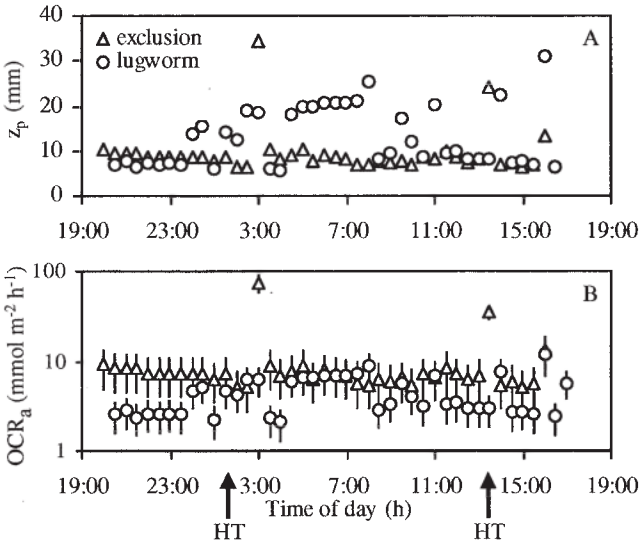

Fig. 8. (A) Oxygen penetration depth on the exclusion and lugworm sites as a function of time determined from in situ microprofiles measured during night and daytime over two subsequent submersion periods (April 2004). In situ oxygen penetration under calm field conditions appeared to be higher and more variable at the lugworm site. (B) Temporal dynamics of areal OCR calculated by combining the in situ oxygen penetration depths and the OCR measurements by the flow-through method (Fig. 5A). The two high OCR_a values in the exclusion site shortly after high tide (HT) correspond to the elevated O_2 penetration depths at these times, possibly indicating bioventilation events. Arrows indicate the time of the high tide (HT).

et al. 2000). Low microphytobenthic biomass may thus have contributed to the reduced silt accretion at the lugworm site. The lower microphytobenthic biomass may be caused by the lugworm feeding activity, since microphytobenthos is a major component in the diet of *A. marina* (Andresen and Kristensen 2002). Additionally, low nutrient concentrations in the pore water may have caused lower microphytobenthic growth (Posey et al. 2002). Van de Koppel et al. (2001) suggested alternate stable states of intertidal flats, where one state is characterized by high diatom cover and high silt content, while the other state is dominated by erosion with low diatom cover and silt content. In this context, the presence of lugworms seems to favor the second state. Surprisingly, higher Chl *a* content in surface sediment of the exclusion site did not result in increased gross photosynthesis rates, presumably indicating an accumulation of photosynthetic inactive Chl *a* of dead microphytobenthic cells at the lugworm exclusion site or dissolved inorganic carbon limitation due to reduced advective exchange (Cook and Røy 2006).

The accumulation of fine material at the lugworm exclusion site was not restricted to the sediment surface but resulted in an increased incorporation and consolidation of this material in the subsurface sediment, forming a conspicuous sticky organic-rich sediment layer in 4–7-cm depth. This incorporation of fine material may be caused by advective cotransport (Rusch and Huettel 2000) and biogenic activities of benthic organisms. High abundances of tentaculate polychaetes like *P. elegans* were present during all years of this study, especially at the exclusion site (Volkenborn and Reise 2007). These polychaetes are capable of enhancing particle removal from the water column and from the sediment surface, and their tubes may function as small sediment traps, bringing fine material to depths of 3–5 cm (Bolam and Fernandes 2003). Increased abundances of the partly suspension-feeding polychaete *N. diversicolor* on the lugworm exclusion plot in the first year of the experiment (Volkenborn and Reise 2006; this study) may have also contributed to increased accumulation and consolidation of fine material (Davey 1994). Thus, the observed changes in sediment characteristics are possibly not due to the absence of *A. marina* alone, but may be enhanced by other abundant benthic species responding to the experimental treatment. These demographic aspects emphasize a complex interplay of biological, physical, and chemical processes. Even though the underlying mechanisms of sediment clogging remain partly speculative, our results show interesting parallels to investigations by Goñi-Urriza et al. (1999), who also observed higher fine particle and organic content within a lugworm exclusion area of 2 × 8 m established by a wooden wreck buried in 10-cm depth.

The observed changes in sediment characteristics had significant implications for the delivery of oxygen into the sediment. For the determination of OCR_a, we used a combination of different in situ and ex situ techniques (Table 3). In situ areal oxygen consumption rates were very variable in time (2.4–9.0 mmol m^{-2} h^{-1}) but well within the range found in other field studies (e.g., Wenzhoefer and Glud 2004). In sediment core incubations with low stirring speeds, the measured fluxes can be assumed to be the diffusive fluxes. These fluxes were four- to fivefold lower than the fluxes calculated by the combination of the in situ oxygen penetration under calm field conditions and the volumetric oxygen consumption rates measured by planar optodes. The discrepancy between sediment core incubation and in situ oxygen fluxes emphasizes the importance of advection induced by hydrodynamic forcing (Huettel and Gust 1992). The exclusion of large macrofauna in incubated sediment cores may have also contributed to the lower OCR_a (Glud et al. 2003).

We suggest that the effects of lugworm-induced changes of the sediment characteristics on oxygen exchange processes depend on the hydrodynamic conditions. In sediment core incubations, where hydrodynamic forcing was minimal, areal sedimentary OCR were slightly higher at the lugworm exclusion site. This was an anticipated result, since the generally more reduced and organic-enriched character of the sediment at the exclusion site is likely to increase diffusive oxygen consumption due to the reoxidation of accumulated reduced compounds and increased organic mineralization (Banta et al. 1999; Papaspyrou et al. 2007). Considering the low oxygen penetration measured in situ at the exclusion site, sedimentary oxygen consumption occurs in a relatively thin active sediment layer. On the other hand, oxygen consumption at the lugworm site occurred in a thicker sediment layer with a generally lower volume-specific oxygen demand. At increased hydrostatic pressure, much deeper oxygen penetration at the lugworm site overcompensated for the lower volumetric oxygen

Table 2. Dominant macrobenthic species at the exclusion, control, and subtidal sites. Shown are mean abundances and standard deviations of August samplings ($n=10$) in three consecutive years. Listed species contributed cumulatively more than 80% to within-site assemblage similarity (SIMPER analysis). Asterisks indicate significantly higher species abundance as revealed by analysis of variance (ANOVA) statistics of exclusion and lugworm site data (* $p<0.05$; ** $p<0.01$; *** $p<0.001$). SD, standard deviation.

Year	Site	Species	Individuals (100 cm)$^{-2}$	SD	ANOVA statistics	Contribution to assemblage similarity (%)
2002	Exclusion	*Nereis diversicolor*	16.4	4.1	***	44
		Pygospio elegans	16.8	9.9	**	30
		Polydora cornuta	6.4	4.1	***	11
	Lugworm	*Tubificoides benedii*	4.2	3.1		37
		Nereis diversicolor	1.2	0.6		16
		Capitella capitata	1.7	1.3	**	15
		Scoloplos cf. *armiger*	1.6	1.6		11
	Subtidal	no data				
2003	Exclusion	*Nereis diversicolor*	8.4	4.5		47
		Polydora cornuta	3.8	2.1	*	21
		Macoma balthica	2.0	1.5		11
		Tharyx marioni	2.6	2.4		9
	Lugworm	*Nereis diversicolor*	8.5	4.0		47
		Macoma balthica	3.5	1.6		19
		Scoloplos cf. *armiger*	2.3	1.6	*	10
		Pygospio elegans	2.5	2.3		9
		Polydora cornuta	1.5	1.6		4
	Subtidal	*Scoloplos* cf. *armiger*	4.0	1.3		48
		Spio martinensis	4.9	3.5		37
		Pygospio elegans	1.5	1.7		7
2004	Exclusion	*Hydrobia ulvae*	97.8	25.2	***	53
		Mya arenaria	34.9	7.2	***	20
		Macoma balthica	27.9	9.0		14
		Lanice conchilega	5.5	2.1	***	3
		Scoloplos cf. *armiger*	6.5	3.9		3
	Lugworm	*Hydrobia ulvae*	30.5	16.3		41
		Macoma balthica	21.6	13.0		26
		Scoloplos cf. *armiger*	10.6	5.0		15
		Cerstaoderma edule	5.8	3.2		7
		Nereis diversicolor	3.8	1.4	*	6
	Subtidal	*Scoloplos* cf. *armiger*	0.5	0.4		100

uptake rates and may have resulted in significantly higher areal uptake rates (*see also Fig. 6B*). Flushing events, e.g., by intense wave action during stormy periods, will thus permit efficient oxidative mineralization of organic material and removal of degradation products from deeper sediment layers and may be one reason that the lugworm tidal flat shared the low organic character of the subtital, more exposed sand. Interestingly, the spatial variability of the areal OCR in sediment core incubations was higher at the exclusion site, while the temporal variability of the areal OCR, calculated from in situ oxygen penetration and volumetric OCR, was higher at the lugworm site. The spatial variability of the areal OCR at the exclusion site reflects the inhomogeneous delivery of oxygen to subsurface sediment layers. With increasing hydrostatic pressures, surface water entered the sediment at the exclusion site mainly via burrow structures (Fig. 7A). In contrast, the oxygen-rich water percolated through the entire sediment volume at the lugworm site (Fig. 7B). The temporal variability of the areal OCR at the lugworm site indicates a higher susceptibility to physical and biological advection, resulting in dynamic oxygen penetration during inundation (Werner et al. 2006).

Table 3. Comparison of sedimentary areal oxygen consumption rates (OCR_a) at the exclusion and the lugworm sites based on different measurements. The diffusive oxygen flux was measured by sediment core incubations. Fluxes under calm field conditions were calculated by combining the oxygen penetration depths measured in situ and volumetric oxygen consumption rates measured ex situ by planar optode imaging. Potential oxygen fluxes during stormy conditions were estimated by combining oxygen penetration under high hydrostatic pressures (~30-cm water column) and the volumetric oxygen consumption rates measured with planar optode imaging. Note that SD of the diffusive flux reflects the spatial variability of OCR_a between individual cores, while SD of the flux under calm field conditions reflects the temporal variability of OCR_a during two subsequent submersion periods. The two extraordinarily high bioirrigative events at the lugworm exclusion site (*see text and Fig. 8*) were omitted from the calculation of calm condition fluxes.

	OCR_a (mmol m^{-2} h^{-1})	
	Exclusion (mean±SD)	Lugworm (mean±SD)
Diffusive flux	1.4±0.3	1.2±0.1
Calm field conditions	7.1±1.5	4.5±2.3
Stormy conditions	<10	>15

The observed differences in sediment characteristics and exchange processes are not independent of each other. We do not regard each as separate evidence but as interacting variables that indicate a cohesive organic-enriched sediment character in the absence, compared to permeable organic-poor sand in the presence, of *A. marina*. We conclude that the effect of large burrowing macrofauna is closely linked to the hydrodynamic regime. Large-scale in situ approaches are necessary to detect the full spectrum of bioturbation and bioirrigation effects on the seafloor (Biles et al. 2002) because results may diverge from those found in the laboratory (e.g., Papaspyrou et al. 2007). At least in semi-exposed fine sands, where a pit-and-mound topography generated by bioturbating infauna is frequently obliterated by water movements, the continuous bioturbation may lead to the maintenance of high sediment permeability that facilitates elevated benthic–pelagic fluxes and thereby affects sedimentary habitat characteristics.

References

Aller, R. C. 1998. Benthic fauna and biogeochemical processes in marine sediments: The role of burrow structures, p. 301–338. *In* T. H. Blackburn and J. Sørensen [eds.], Nitrogen cycling in coastal marine environments. Wiley.

Andresen, M., and E. Kristensen. 2002. The importance of bacteria and microalgae in the diet of the deposit-feeding polychaete *Arenicola marina*. Ophelia **56:** 179–196.

Austen, I. 1994. The surficial sediments of Königshafen—variations over the past 50 years. Helgol. Meeresunters. **48:** 163–171.

Banta, G. T., M. Holmer, M. H. Jensen, and E. Kristensen. 1999. Effects of two polychaete worms, *Nereis diversicolor* and *Arenicola marina*, on aerobic and anaerobic decomposition in a sandy marine sediment. Aquat. Microb. Ecol. **19:** 189–204.

Beukema, J. J. 1976. Biomass and species richness of the macrobenthic animals living on the tidal flats of the Dutch Wadden Sea. Neth. J. Sea Res. **10:** 236–261.

Biles, C. L., D. M. Paterson, R. B. Ford, M. Solan, and D. G. Raffaelli. 2002. Bioturbation, ecosystem functioning and community structure. Hydrol. Earth Syst. Sci. **6:** 999–1005.

Bolam, S. G., and T. F. Fernandes. 2003. Dense aggregations of *Pygospio elegans* (Claparede): Effect on macrofaunal community structure and sediments. J. Sea Res. **49:** 171–185.

Cadée, G. C. 1976. Sediment reworking by *Arenicola marina* on tidal flats in the Dutch Wadden Sea. Neth. J. Sea Res. **10:** 440–460.

Cook, P. L. M., and H. Røy. 2006. Advective relief of CO_2 limitation in microphytobenthos in highly productive sandy sediments. Limnol. Oceanogr. **51:** 1594–1601.

D'Andrea, A. F., R. C. Aller, and G. R. Lopez. 2002. Organic matter flux and reactivity on a South Carolina sandflat: The impacts of pore water advection and macrobiological structures. Limnol. Oceanogr. **47:** 1056–1070.

Davey, J. T. 1994. The architecture of the burrow of *Nereis diversicolor* and its quantification in relation to sediment-water exchange. J. Exp. Mar. Biol. Ecol. **179:** 115–129.

De Beer, D., F. Wenzhoefer, T. G. Ferdelman, S. E. Boehme, M. Huettel, J. E. E. van Beusekom, M. E. Böttcher, N. Musat, and N. Dubilier. 2005. Transport and mineralization rates in North Sea sandy intertidal sediments, Sylt-Rømø Basin, Wadden Sea. Limnol. Oceanogr. **50:** 113–127.

De Jonge, V. N. 1980. Fluctuations in the organic carbon to chlorophyll a ratios for estuarine benthic diatom populations. Mar. Ecol. Prog. Ser. **2:** 345–353.

Fenchel, T., and B. J. Finlay. 1995. Ecology and evolution in anoxic sediments. Oxford Univ. Press.

Fonselius, S. 1983. Determination of hydrogen sulfide, p. 134–137. *In* K. Grasshoff, M. Ehrhardt and K. Kremling [eds.], Methods of Seawater Analysis. Verlag Chemie.

Glud, R. N., J. K. Gundersen, H. Røy, and B. B. Jørgensen. 2003. Seasonal dynamics of benthic O_2 uptake in a semi enclosed bay: Importance of diffusion and faunal activity. Limnol. Oceanogr. **48:** 1265–1276.

———, N. B. Ramsing, J. K. Gundersen, and I. Klimant. 1996. Planar optodes, a new tool for fine scale measurements of two-dimensional O_2 distribution in benthic communities. Mar. Ecol. Prog. Ser. **140:** 217–226.

Goñi-Urriza, M., X de Montaudouin, R. Guyoneaud, G. Bachelet, and R de Wit. 1999. Effect of macrofaunal bioturbation on bacterial distribution in marine sandy sediments, with special reference to sulphur-oxidising bacteria. J. Sea Res. **41:** 269–279.

Grant, J., U. V. Bathmann, and E. L. Mills. 1986. The interaction between benthic diatom films and sediment transport. Estuar. Coast. Shelf Sci. **23:** 225–238.

Holst, G., and B. Grunwald. 2001. Luminescence lifetime imaging with transparent oxygen optodes. Senssor. Actuat. B. Chem. **74:** 78–90.

Huettel, M. 1990. Influence of the lugworm *Arenicola marina* on porewater nutrient profiles of sand flat sediments. Mar. Ecol. Prog. Ser. **62:** 241–248.

———, and G. Gust. 1992. Impact of bioroughness on interfacial solute exchange in permeable sediments. Mar. Ecol. Prog. Ser. **89:** 253–267.

———, W. Ziebis, S. Forster, and G. W. Luther III. 1998. Advective transport affecting metal and nutrient distributions and interfacial fluxes in permeable sediments. Geochim. Cosmochim. Acta **62:** 613–631.

Hylleberg, J. 1975. Selective feeding by *Abarenicola pacifica* with notes on *Abarenicola vagabunda* and a concept of gardening in lugworms. Ophelia **14:** 113–137.

Jeroschewski, P., C. Steukart, and M. Kuehl. 1996. An amperometric microsensor for the determination of H_2S in aquatic environments. Anal. Chem. **68:** 4351–4357.

Klute, A., and C. Dirksen. 1986. Hydraulic conductivity and diffusivity: Laboratory methods, p. 687–700. *In* A. Klute [ed.], Methods of Soil Analysis. Part 1—Physical and Mineralogical Methods. American Society of Agronomy.

Kristensen, E. 1988. Benthic fauna and biogeochemical processes in marine sediments: Microbial activities and fluxes, p. 275–299. *In* T. H. Blackburn and J. Sørensen [eds.], Nitrogen Cycling in Coastal Marine Environments. Wiley.

Lorenzen, C. J. 1967. Determination of chlorophyll and pheopigments: Spectrophotometric equations. Limnol. Oceanogr. **12:** 343–346.

Mackin, J. E., and K. T. Swider. 1989. Organic matter decomposition pathways and oxygen consumption in coastal marine sediments. J. Mar. Res. **47:** 681–716.

Malcolm, S. J., and D. B. Sivyer. 1997. Nutrient recycling in intertidal sediments, p. 59–99. *In* T. D. Jickells and J. E. Rae [eds.], Biogeochemistry of Intertidal Sediments. Cambridge Univ. Press.

Papaspyrou, S., E. Kristensen, and B. Christensen. 2007. *Arenicola marina* (Polychaeta) and organic matter mineralization in sandy marine sediments: In situ and microcosm comparison. Estuar. Coast. Shelf Sci. **72:** 213–222.

Paterson, D. M. 1989. Short-term changes in the erodibility of intertidal cohesive sediments related to the migratory behavior of epipelic diatoms. Limnol. Oceanogr. **34:** 223–234.

POLERECKY, L., U. FRANKE, U. WERNER, B. GRUNWALD, AND D. DE BEER. 2005. High spatial resolution measurement of oxygen consumption rates in permeable sediments. Limnol. Oceanogr. Methods **3:** 75–85.

POSEY, M., T. ALPHIN, L. CAHOON, D. LINDQUIST, M. MALLIN, AND M. NEVERS. 2002. Top-down versus bottom-up limitation in benthic infaunal communities: Direct and indirect effects. Estuaries **25:** 999–1014.

REISE, K. 1985. Tidal flat ecology. Springer.

———. 2002. Sediment mediated species interactions in coastal waters. J. Sea Res. **48:** 127–141.

REVSBECH, N. P. 1989. An oxygen microelectrode with a guard cathode. Limnol. Oceanogr. **55:** 1907–1910.

RIISGÅRD, H. U., AND G. T. BANTA. 1998. Irrigation and deposit feeding by the lugworm *Arenicola marina*, characteristics and secondary effects on the environment. A review of our current knowledge. Vie Milleu **48:** 243–257.

RUSCH, A., AND M. HUETTEL. 2000. Advective particle transport into permeable sediments—evidence from experiments in an intertidal sandflat. Limnol. Oceanogr. **45:** 525–533.

THAMDRUP, B., AND D. E. CANFIELD. 2000. Benthic respiration in aquatic systems, p. 86–103. *In* O. E. R. Sala, R. B. Jackson, H. A. Mooney and R. W. Horwarth [eds.], Methods in ecosystem science. Springer.

TIMMERMANN, K., G. T. BANTA, AND R. N. GLUD. 2006. Linking *Arenicola marina* irrigation behavior to oxygen transport and dynamics in sandy sediments. J. Mar. Res. **64:** 915–938.

VAN DE KOPPEL, J., P. M. J. HERMAN, P. THOOLEN, AND C. H. R. HEIP. 2001. Do alternate stable states occur in natural ecosystems? Evidence from a tidal flat. Ecology **82:** 3449–3461.

VOLKENBORN, N., AND K. REISE. 2006. Lugworm exclusion experiment: Responses by deposit feeding worms to biogenic habitat transformations. J. Exp. Mar. Biol. Ecol. **330:** 169–179.

———, AND K. REISE. 2007. Effects of *Arenicola marina* on polychaete functional diversity revealed by large-scale experimental lugworm exclusion. J. Sea Res. **57:** 78–88.

WENZHOEFER, F., AND R. N. GLUD. 2004. Small-scale spatial and temporal variability in coastal benthic O_2 dynamics: Effects of fauna activity. Limnol. Oceanogr. **49:** 1471–1481.

WERNER, U., M. BILLERBECK, L. POLERECKY, U. FRANKE, M. HUETTEL, J. E. E. VAN BEUSEKOM, AND D. DE BEER. 2006. Spatial and temporal patterns of mineralization rates and oxygen distribution in a permeable intertidal sand flat (Sylt, Germany). Limnol. Oceanogr. **51:** 2549–2563.

WETHEY, D. S., AND S. A. WOODIN. 2005. Infaunal hydraulics generate porewater pressure signals. Biol. Bull. **209:** 139–145.

YALLOP, M. L., D. M. PATERSON, AND P. WELLSBURY. 2000. Interrelationships between rates of microbial production, exopolymer production, microbial biomass, and sediment stability in biofilms of intertidal sediments. Microb. Ecol. **39:** 116–127.

ZIEBIS, W., M. HUETTEL, S. FORSTER, AND B. B. JØRGENSEN. 1996. Complex burrows of the mud shrimp *Callianassa truncata* and their geochemical impact in the sea bed. Nature **382:** 619–622.

Received: 16 January 2007
Accepted: 5 April 2007
Amended: 26 April 2007